13th World Conference on Earthquake Engineering
Vancouver, B.C., Canada
August 1-6, 2004
Paper No. 2123

NUMERICAL ANALYSIS OF LIQUEFACTION-INDUCED LATERAL SPREADING

Abbas SOROUSH [1] and Sheila KOOHI [2]

SUMMARY

Liquefaction-induced lateral spreading of saturated sandy deposits happen during and shortly after earthquakes. This paper first reviews this important phenomenon by means of reviewing observations on case histories and experimental works of lateral spreading. Then numerical analysis of the lateral spreading of the Wildlife Site, Imperial Valley, California, which happened during the 1987 Superstition Hills Earthquake, is numerically analyzed. Three types of analysis are carried out: a) coupled liquefaction-consolidation analysis using the coefficient of permeability (K_1) of the liquefied layers, as reported in the literature; b) analysis type (a), but with K equal to 0.1 of K_1, and c) a fully undrained liquefaction analysis. The analyses results in forms of excess pore water pressures and surface displacements indicated that the fully undrained behavior of the liquefied layers better represents the behavior and response of the site during the earthquake.

INTRODUCTION

Liquefaction-induced lateral displacements, which happen in saturated sandy deposits, cause significant damages during and some times after earthquakes. This phenomenon has caused damages to the foundations of buildings, bridges, embankments, canals and lifeline facilities. These displacements are usually permanent and range from a few centimeters to a few meters. Lateral displacements usually occur in the vicinity of free boundaries such as small creeks, rivers and quay walls.

In the 1906 San Francisco Earthquake, lateral spreading of the ground caused fire and interruption of water pipes [1]. In the 1964 Alaska Earthquake, hundreds of million dollars damage was inserted to more than 250 bridges due to lateral displacement of the ground [2]. The one billion dollar damage in 1964 Nigata Earthquake can also be related to lateral spreading [3]. The reported lateral spreading in this earthquake was more than 10 meters [4]. Considerable damages due to liquefaction and lateral spreading in the 1971 San Fernando Earthquake, the 1990 Lozan Earthquake, the 1990 Manjil Earthquake and the

[1] Assistant Professor, Department of Civil and Environmental Engineering, Amirkabir University of Technology, Tehran, Iran, Email: soroush@aut.ac.ir
[2] Former M. Sc. Student, Department of Civil and Environmental Engineering, Amirkabir University of Technology, Tehran, Iran.

1991 Costa Rica Earthquake have also been reported [5; 6]. The 1995 Hykogen Nambu Earthquake (Kobe, Japan) caused 100 billion dollars damage, mostly by liquefaction and lateral spreading. Also the collapse of some buildings in the recent earthquakes of Turkey and Taiwan must be due to this phenomenon.

This paper reviews some of lateral spreading case histories and experimental studies on the phenomenon. Then a numerical analysis of the liquefaction-induced lateral spreading of the Wildlife Site, during the 1987 Superstition Hills Earthquake, will be introduced. The analyses have been carried out using the Computer Code FLAC. Results of the analyses are compared with the recorded responses of the site.

OBSERVATIONS ON CASE HISTORIES

A review on the happened lateral spreading in Nigata (1964), San Fernando (1983), Manjil (1990) and other earthquakes, in which lateral spreading has occurred, resulted in a number of observations as follows:

- Liquefaction and the resulting lateral spreading usually happen in alluvial plains containing loose sandy soils.
- A loose liquefiable layer (N-SPT < 10) has been present in all cases [7].
- Liquefied soils have displaced from higher elevations to lower elevations, indicating that gravity plays an important role in lateral spreading.
- A meaningful relationship is present between the displacements of the ground and the thickness of the liquefied soil.
- In many cases, ground displacements continued sometimes after the earthquakes [4].

OBSERVATIONS ON LABORATORY TESTING

Extensive laboratory tests, including shaking table and centrifuge testing have been carried out by many researchers to study liquefaction and lateral spreading. A thorough review on the laboratory tests results yields the following conclusions [4; 8; 9]:

- Pore pressures increase during dynamic loading; having approached a (u/σ_v) 1.0, then the displacements triggers in the direction of the slope.
- Deformations occur in the liquefied layer; the above non-liquefiable layer (if present) moves due to the movement of the liquefied layer.
- Pore pressures remain constant after the end of the vibration; then they dissipate gradually. Displacements in the ground stop by the end the vibration.
- The direction of lateral spreading is independent of the direction of vibration. The displacements happen in the direction of the maximum ground surface gradient. The higher the surface gradient, the more the lateral spreads.
- In shaking table tests, the displacements have the maximum amount at the surface and the minimum (almost zero) at the bottom of the layer.

COMPARISON OF LABORATORY AND FIELD RESULTS

The main difference between lateral spreading in the laboratory tests and the real earthquakes is the continuation of the displacements in the real earthquakes after the end of the earthquake. The latter process is named the “delayed response” in liquefaction effects in the literature [10]. Mainly, two factors have been proposed for the mentioned difference [10; 11]. In small shaking table tests, due to small sizes of the models, a very short time is needed for the occurrence of liquefaction and displacements and the

entire displacements end by the end of the dynamic loading. However in real earthquakes, a large amount of soil is shaken for a very small duration. Occurrence of stress redistribution, pore water pressure redistribution – according to the volume of the soil mass and the complexity of boundary conditions- in a short period of time is not possible. Therefore, long times after the end of the earthquake, the displacements will continue and yield large displacements. Another reason is that in most laboratory models, due to the shaking process, liquefaction occurs in the early stages of loading and due to the boundary conditions, some of the consolidation process might happen in these stages as well. Therefore, the residual strength of the liquefied soil at the end of the earthquake would increase and the displacements stop. In real earthquakes, maximum excess pore water pressures would happen at final seconds of the earthquakes and, therefore, there is no time for consolidation and increase in the residual strength [12]. Figure 1 shows a summary of geotechnical stages involved during and after earthquakes.

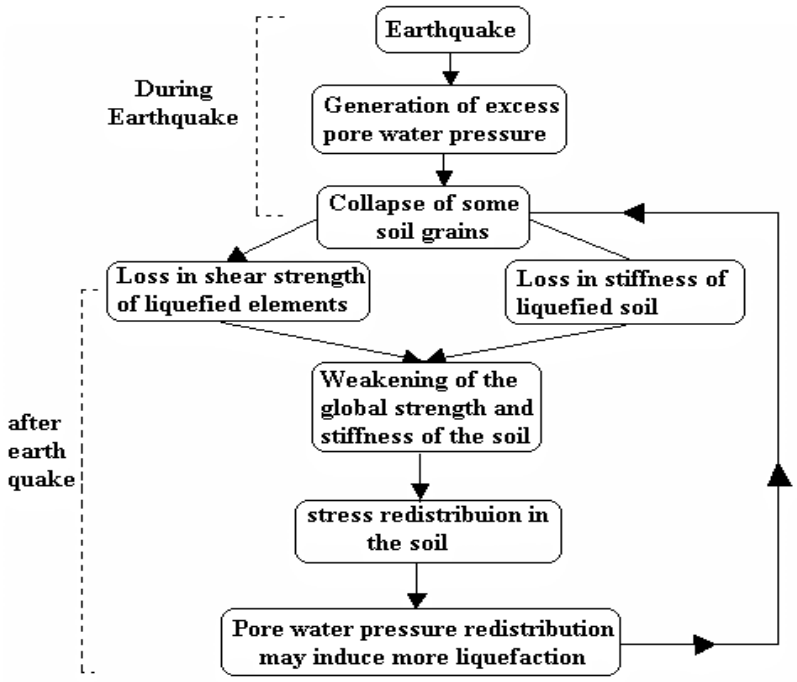

Figure 1. A summary of geotechnical stages during and after the earthquake

DESCRIPTION OF THE WILDLIFE LIQUEFACTION SITE

An earthquake of magnitude M_s = 6.0 on April 26, 1981 in the Imperial Valley near Westmorland, California, caused a significant amount of damage, in many cases by liquefaction and lateral spreading. This prompted a detailed geological survey of the valley and the selection of a site for the installation of accelerometers and piezometers to record ground motions and pore water pressure changes during future earthquakes. The site chosen was the Wildlife Management Area located 3km south of Calipatria in the Imperial Wildfowl Management Area and lying on the west side of the incised flood plain of the Alamo River. Figure 2 presents a plan view of the site, in which sand boils and lateral spreading are shown.

Penetration tests and samples, taken by the U.S. Geological Survey [13], identified seven geological units in the upper 26.5m. Of these seven layers, the three topmost units were considered to be the most significant as they lie within a zone of high liquefaction probability. A section across the flood plain showing these three units and the arrangement of the instrumentation are shown in Figure 3. The

instrumentation was installed in 1982 and consisted of surface and down-hole (7.5m depth) accelerometers and 6 pore-water pressure transducers.

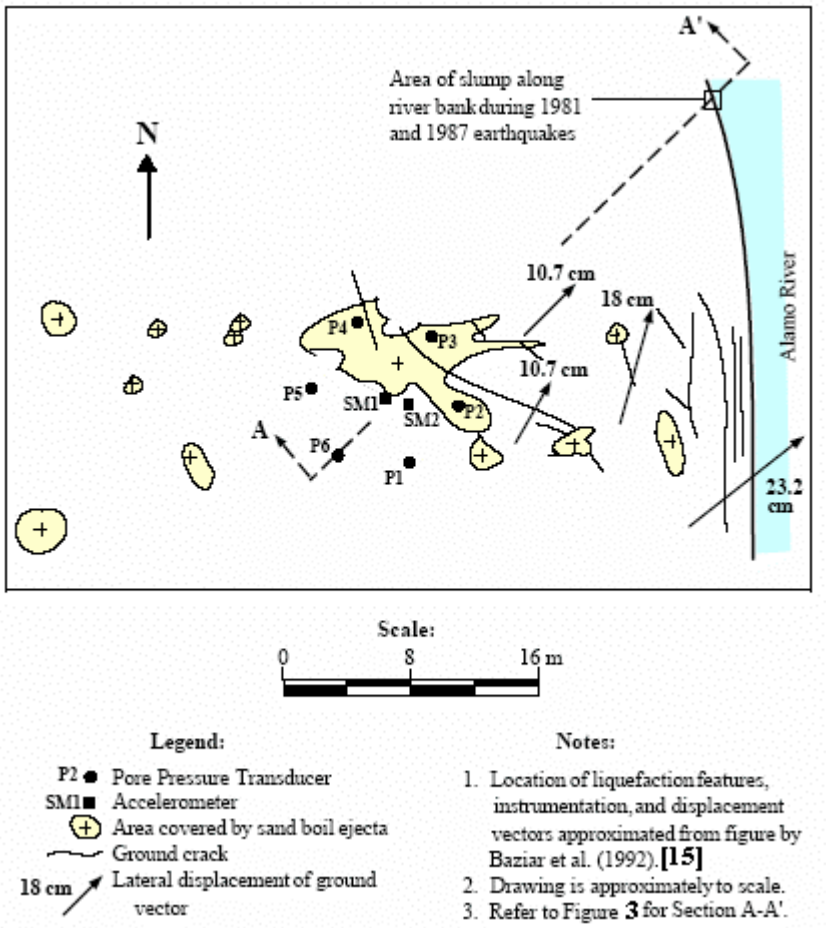

Figure 2: Plan of sand boils, lateral spreading, and cracks at Wildlife Liquefaction Site after 1987 Superstition Hills Earthquake [16]

Within the upper three units, a closer examination by Holzer et al. [14] revealed five geological soil strata to the level of the downhole accelerometer, as presented in Figure 3. The profile generally consists of about 2.5 meters of very loose silt underlain by 1 meter of very loose sandy silt, and about 3.3 meters of loose silty sand to very fine sand. Beneath the silts and sands are about 0.7 meters of medium to stiff clayey silt. The border of the site is a river whose bottom is approximately 4.9 meters below the adjacent ground surface. The groundwater and river levels are approximately 1.2 meters below ground surface.

Five years after the instrumentation of the site, two earthquakes with medium magnitudes and two post earthquakes caused responses in the instruments in the site. The first earthquake, Elmore Ranch Earthquake, with a magnitude of 6.3 occurred on 23rd of Nov. 1987 and caused some changes in pore pressures. The second earthquake, namely Superstitions Hills Earthquake, with a magnitude of 6.7 happened on 24th of Nov. 1987 and caused liquefaction and lateral spreading in the site. The acceleration time history of the latter earthquake is shown in Figure 4.

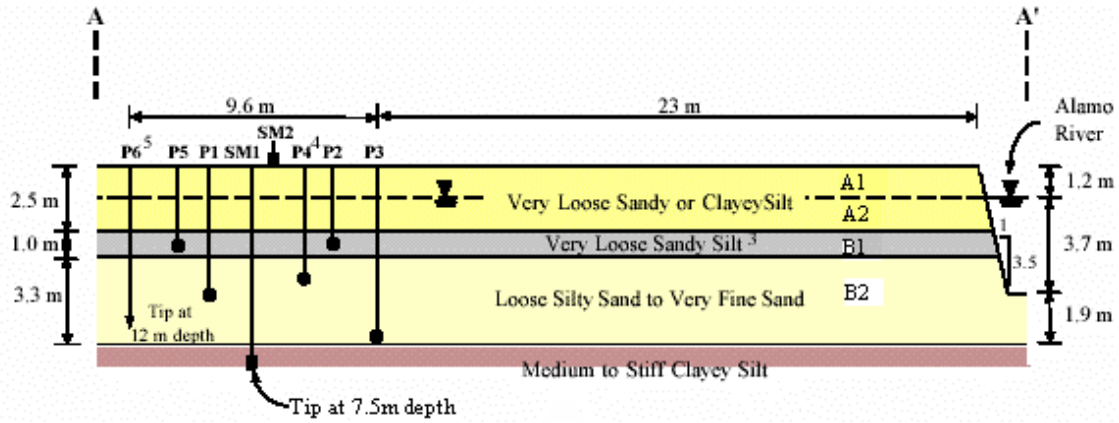

P2 : Piezometer (Pore pressure transducer)

SM1 : Accelerometer (horizontal and Vertical)

1. Instruments are offset perpendicular to section line A-A' as shown on Figure 2
2. Profile based on information provided in Baziar et al. (1992) for vicinity of instrument array. Profile assumed to be same between instrument array and river [15].
3. Sandy silt layer also described as silty sand layer in Baziar et al.
4. No data provided in Baziar et al. for piezometer P4 [15].
5. Tip of piezometer P6 located in silt layer at 12 m depth.

Figure 3: Section AA' showing soil profile and instrumentation at Wildlife Liquefaction Site [16]

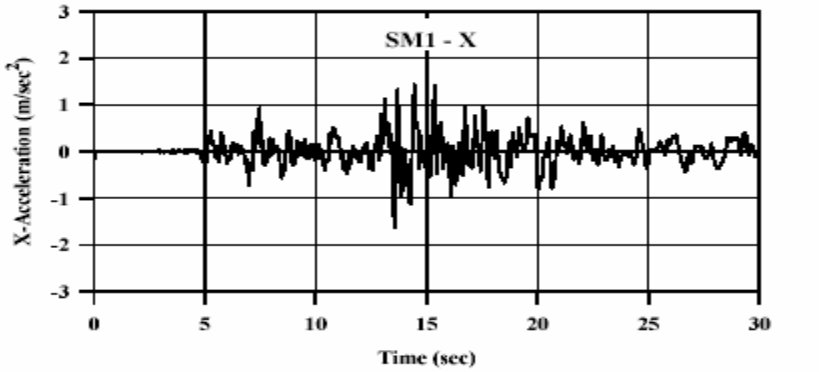

Figure 4. Time history of the Superstition Hills earthquake acceleration [16]

The lateral displacements measured at the ground surface of the Wildlife Site after the Superstition Hills Earthquake ranged from 10.7 to 23.2cm toward the river, as shown in Figure 2. It is seen that the displacements are larger in the vicinity of the river bank [16].

Figure 5 compiles responses of piezometers P1, P2, P3 and P5 during and shortly after the earthquake. Since piezometer P4 didn't function properly [17] and piezometer P6 was located at a depth of 12m (Figure 3), where no liquefiable layer is present, they are not included in Figure 5. It is observed that the excess pore water pressure in piezometer P3 (depth 6.28 m) rises up to 61kPa at 60 sec and 67kPa at 90 sec after the beginning of the earthquake. Piezometers P2 and P5 are almost at a same depth (2.9 and 3.0 m) and have a same trend of increase in excess pore water pressures to 38kPa at 90 seconds. Piezometer P1 is located at a depth of 5.0m, where the pore pressure has risen to 58kPa at 90 seconds.

It is observed from Figure 5 that excess pore water pressures at any time increase according to depth; i.e., the deeper the location of the piezometer, the higher the induced excess pore water pressure, This fact has resulted in an upward hydraulic gradient, and consequently an upward flow. The presence of the sand

boils in the surface can be explained by this phenomenon. It is interesting that the pore water pressure buildup in different piezometers continued even after the end of the peak acceleration of the earthquake ($t_{eq.}$=20). This continuation of the piezometers responses, namely delayed response, as discussed in the previous section, is an important phenomenon. Table 1 shows normalized pore water pressures at the piezometers during and after the end of the peak acceleration of the earthquake. It is observed that layers A2, B1 and B2 have reached zero effective stress state and have been liquefied at 90 seconds.

NUMERICAL ANALYSIS OF THE WILDLIFE SITE

Computer Code

We selected a computer code for numerical analyses of lateral spreading based primarily on:

- ability to introduce time-acceleration history of an earthquake to the analysis,
- ability to model and compute excess pore water pressures induced by earthquake,
- ability to analyze and compute large strains, and
- flexibility for adding new formulations for alternative soil behaviors.

The Computer Code FLAC (Fast Lagrangian Analysis of Continua) was found to have the above abilities and therefore, was selected for lateral spreading analyses. FLAC uses an explicit, finite difference formulation for solving geomechanic problems. The version of the code used in this research was FLAC Version 4.0. FLAC has a number of additional features important for modeling of liquefaction problems, including [18]:

- a stable, large strain formulation, and
- the built-in Finn Model which enables one to model liquefaction and to compute pore pressures induced by earthquake.

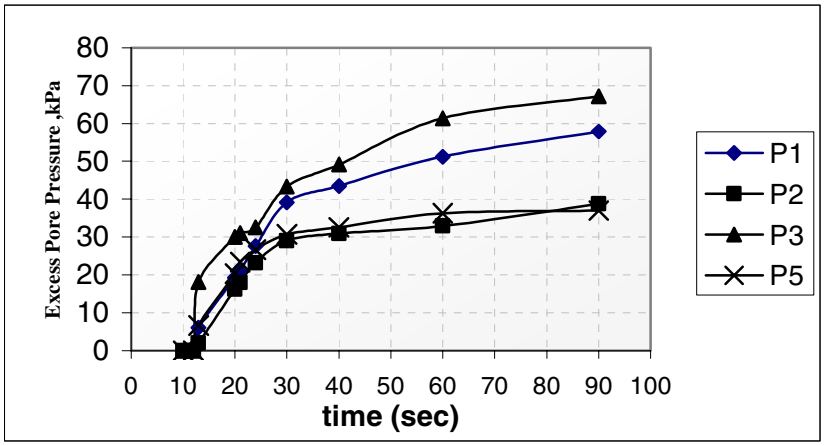

Figure 5. Measured excess pore pressures in different piezomerters at Wildlife Site

Table 1. Normalized pore water pressures at piezometers during and shortly after the earthquake

Piezometer, depth	Measured (u/σ_v)		
	At the end of earthquake (20 sec.)	At 60 sec.	At 90 sec.
P3,6.28m	0.69	0.92	0.96
P1, 5.0m	0.63	0.92	0.98
P5, 2.9m	0.67	0.99	1.00
P2, 3.0m	0.67	0.94	1.00

Finite Difference Grid and Model Properties

The liquefaction and lateral spreading of the Wildlife Site was analyzed numerically using the finite difference grid shown in Figure 6. Computed pore water pressures and surface displacements were monitored in zones and at nodes close to the locations and depths where the instruments were located in the field. The soil properties and stress-strain parameters assigned to the various soil layers modeled in the analysis are summarized in Table 2.

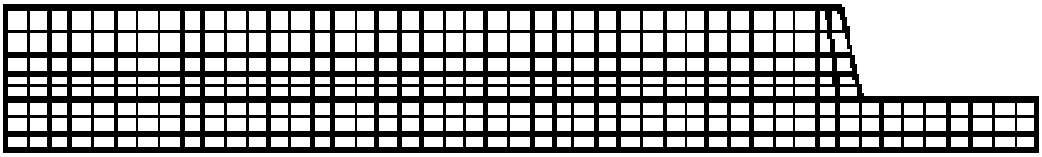

Figure 6. Finite difference idealization for Wildlife Site analysis

Table 2. Material parameters for the layered soil deposits at Wildlife Site

Soil type	Depth (m)	φ' (°)	C' (kPa)	ψ (°)	k (m/s)	E (*10^4 kPa)
Sandy silt	0-1.2 m	28	0	0	$5*10^{-7}$	3.77
Sandy silt	1.2-2.5 m	28	0	0	$5*10^{-7}$	6.032
Sandy silt	2.5-3.5 m	28	0	0	$5*10^{-7}$	7.13
Silty sand to fine sand	3.5-6.8 m	33	0	0	$2.1*10^{-6}$	6.25
Clayey silt to silty clay	6.8-7.5 m	28	48	0	$1*10^{-8}$	8.52

φ' = Effective friction angle
c' = Effective cohesion
ψ = Dilation angle
k = Permeability
E = Elastic modulus

Principles of Finn Model

The Finn Model provided with FLAC for simulating liquefaction uses Mohr-Coulomb failure criteria along with an assumed linear elastic-perfectly plastic stress-strain behavior. The linear elastic behavior is governed by the bulk and shear moduli which can be decreased through the analysis by the user to encounter losses of soil stiffness during liquefaction. Pore water pressure generation is modeled by computing volumetric strains induced by the cyclic shear strains using a formulation given by Martin et al. [19]. In this formulation the volumetric strain increment ($\Delta\varepsilon_v$) occurring in any cycle of loading depends on the shear strain (γ) which occurs during that cycle as well as the previously accumulated volumetric strains (e_v):

$$\Delta\varepsilon_v = C_1 \exp(-C_2 \varepsilon_v/\gamma) \quad (1)$$

where, $\Delta\varepsilon_v$ = volumetric strain increment that occurs over the current cycle,
ε_v = accumulated volumetric strains occurred over the previous cycles,
γ = amplitude of the shear strain for the current cycle, and
C1 and C_2 = constants dependent on the volumetric strain behavior of the sand and are calculated as follows:

$$C_1 = 7600 (D_r)^{-2.5} = 8.7 (N_1)_{60}^{-1.25} \quad (2)$$

$C_2 = 0.4/C_1$ (3),

where, D_r is the relative density of the soil (in percent) and $(N_1)_{60}$ is the SPT test number.

In order to verify the numerical model, we modeled and analyzed numerically the first centrifuge model test of Verification of Liquefaction Analysis by Centrifuge Studies (VELACS). Results of this analysis [20] proved that the Finn Model adopted in the FLAC Computer Code is able to model properly liquefaction and lateral spreading phenomena.

Analysis Procedure for Wildlife Site

First we computed pre-earthquake insitu stresses in the elements of the soil layers. Then we subjected the ground at a depth of 7.5m to the acceleration time history (shown in Figure 4), as we activated the Finn Model in the analysis for computing earthquake-induced pore water pressures and displacements.

Preliminarily sensitivity analyses showed that earthquake-induced pore pressures are very sensitive to the value of coefficient of permeability. Therefore, we performed three types of analyses. a) consolidation analysis using the coefficient of permeability reported in the literature [14] as shown in Table 2, b) consolidation analysis using 0.1 of the coefficient of permeability reported in the literature, and c) fully undrained (i.e., no consolidation) analyses. Results of the analysis are as follows.

Analyses Results

Computed time histories of excess pore water pressure values at the locations of piezometers P1, P2, and P3, for the above three types of analyses (a, b, and c), are compared with the recorded values in Figures 7, 8, and 9, respectively. For Type c Analysis i.e. fully undrained analysis, computed values of displacement history for four different surface points are presented in Fig. 10. Figure 11 compares these values with their associated measured values.

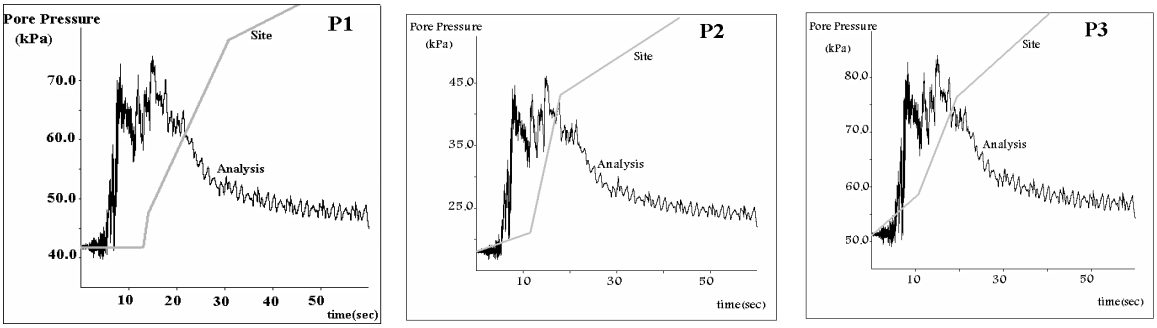

Figure 7. Recorded and computed pore pressure time histories in piezometers (Type a Analysis)

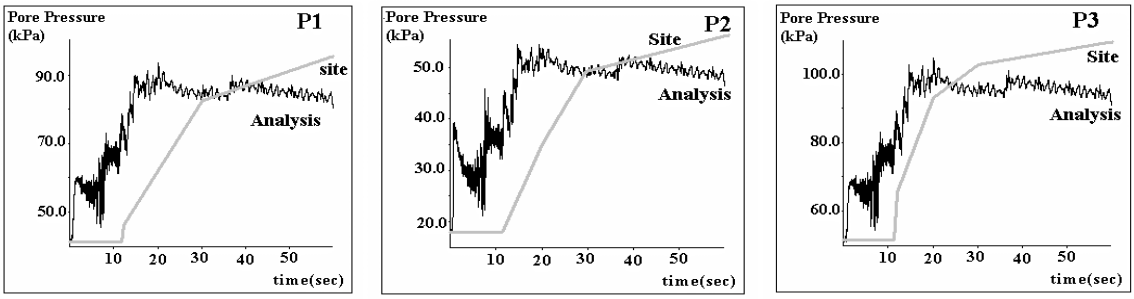

Figure 8. Recorded and computed pore pressure time histories in piezometers (Type b Analysis)

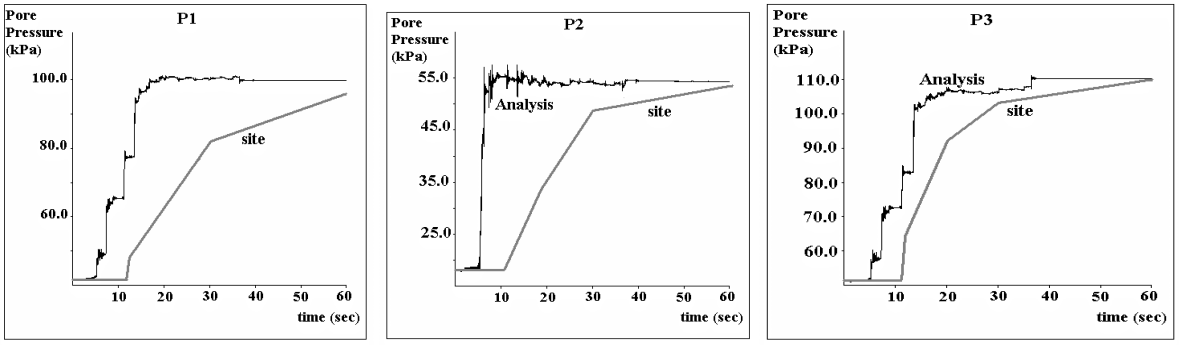

Figure 9. Recorded and computed pore pressure time histories in Piezometers (Type c Analysis)

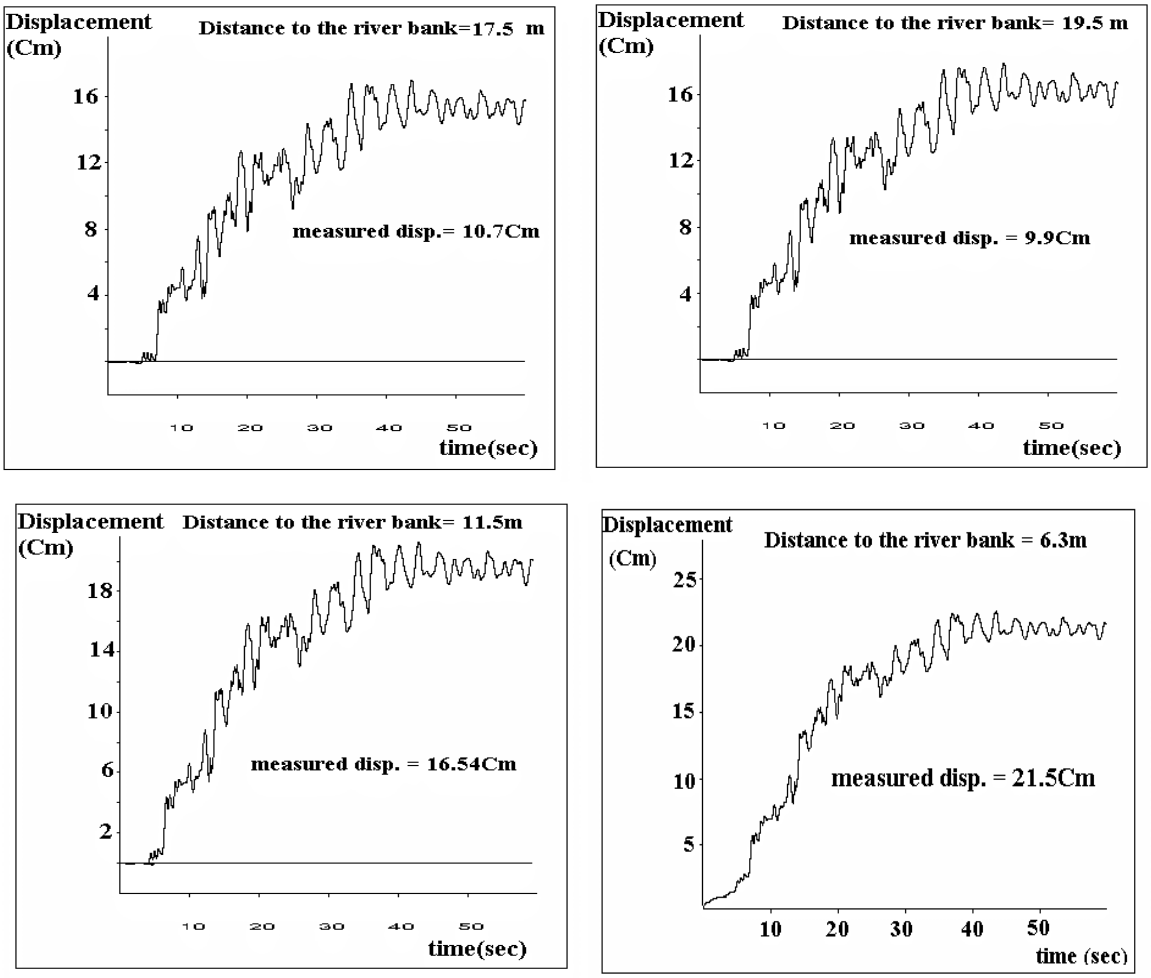

Figure 10. Displacement time history for four surface points (Type c Analysis)

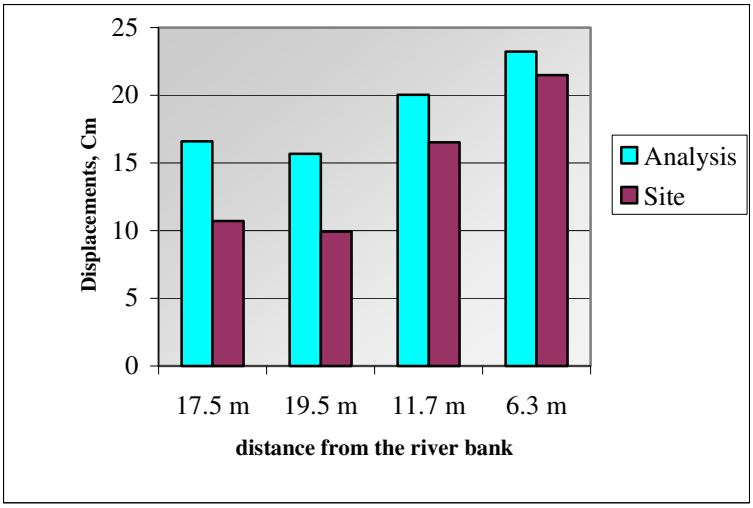

Figure 11. Comparison of computed and measured displacements

Interpretation of the Results

Pore water pressure response

It is observed in Figure 7 that in the coupled liquefaction-consolidation analysis with the reported coefficient of permeability in the literature (Type a Analysis), the general trend of the computed excess pore water pressures are very much different from the monitored pressures in the piezometers. The computed pore pressures increase until they reach a peak amount after about 15 sec; then they start to dissipate and after about 60 sec, they reach residual minimum values. Whereas at this time, the measured excess pore water pressures are still increasing.

As it is obvious in Figure 8, by reducing the coefficients of permeability of the liquefied layers to 0.1 of the coefficients of permeability reported in the literature (Type b Analysis), the post-peak behaviors of the computed and measured excess pore pressures converge together. However, these behaviors are different at pre-peak times of the earthquake. While the measured pressures develop gradually until the final seconds of the acceleration-time history, the computed pressures rise suddenly at about 15 seconds after the beginning of the earthquake and then remain almost constant.

Figure 9 shows that for the fully undrained analysis (Type c Analysis), the computed excess pore water pressure values are comparatively more similar to the measured values. This similarity is evident for both pre-peak and post-peak behavior of the piezometers.

Horizontal displacements

According to Figure 11, the computed maximum surface displacement values are larger than the measured values; however, their differences are not significant. It is well known to the geotechnical profession that a precise computation of field displacement is a challenging and very difficult assignment for almost all areas of geotechnical practice.

CONCLUSIONS

This paper reviewed some observations on case histories of liquefaction-induced lateral spreading of saturated sandy deposits, which occur during earthquakes. Also some observations on laboratory studies of lateral spreading were introduced and discussed. The liquefaction and lateral spreading of the Wildlife Site, during the 1987 Superstition Hills Earthquake, were reviewed and the behaviors of the piezometers

installed in the site were studied and discussed. Finally, the paper introduced a numerical analysis of the lateral spreading at the Wildlife Site. This analysis was carried out using the Computer Code FLAC. Results of the analysis, i.e., excess pore water pressures and surface displacements, indicated that the fully undrained behaviors of the liquefied layers better represents the behavior and responses of the site during the earthquake.

REFERENCES

1. Darragh R.R., Taylore H.T., Scawthorn C., Seidel D., Ng C. "Liquefaction study, Sullivan March and Mission Creek, San Francisco, California". Proceedings of 4th Japan-U.S. Workshop on Earthquake Resistant Design of Lifeline Facilities and Countermeasures for Soil Liquefaction, 1992, vol. 1, 205-221.
2. Doi M., Hamada M. "A summary of case studies on liquefaction-induced ground displacements". Proceedings of 4th Japan-U.S. Workshop on Earthquake Resistant Design of Lifeline Facilities and Countermeasures for Soil Liquefaction, 1992, vol. 1, 115-129.
3. Hamada M., O'Rourke T.D., Yoshida N. "Liquefaction-induced large ground deformation". Performance of Ground and Soil Structures During Earthquakes, 13th ICSMFE, New Delhi, JSSMFE, 1994, 93-108.
4. Hamada M. "Case studies of liquefaction and lifeline performance during past earthquakes.", Technical Report NCEER-92-0001 National Centre for Earthquake Engineering Research, Buffalo, NY., vol.1, Sec.3, 1992.
5. Ishihara K., Takeuchi M. "Flow failure of liquefied sand in large-scale shaking tables". Proceeding of 2nd Int. Conf. on Recent Advances in Geotech. Earthquake Eng. and Soil Dynamics, 1991, 1753-1766.
6. Bartlet S.F., Youd T.L. "Empirical prediction of Lateral spread Displacement." Proceedings of the 4th Japan-U.S. Workshop on Earthquake Resistant Design of Lifeline Facilities and Countermeasures for Soil Liquefaction, Japan, 1992, 351-365.
7. Holzer T.L., Youd T.L., Hanks T.C. "Dynamics of liquefaction during the Superstition Hills Earthquake (M=6.5) of November 24, 1987.", Science 1989; 244: 56-59.
8. Sasaki Y., Tokida K., Matsumoto H., Saya S. "Experimental study on lateral flow of ground due to soil liquefaction". Proceedings of the 2nd Int. Conf. on Recent Advances in Geotech. Earthquake Engrg. and Soil Dynamics, 1991, vol. 1, 263-270.
9. Hamada M., Yasuda S., Isoyama R., Emoto, K., "Study on Liquefaction Induced Permanent Ground Displacements." Association for the Development of Earthquake Prediction: Japan, 1986.
10. Soroush A. Morgenstern, N.R. Robertson P.K. Chan D. "Post-earthquake deformation analysis of the Upper San Fernando Dam," Proceedings of the international symposium on seismic and environmental aspects of dams design: earth concrete and tailings dams, Santiago Chile, October 14-18, 1996 vol. I: 405-418.
11. Gu W.H. "Liquefaction and post-earthquake deformation analysis," Ph. D. Thesis, University of Alberta, 1992.
12. Ishihara K. "Liquefaction and flow failure during earthquakes." Geotechnique 1993, 43(3): 351-415.
13. Bennet M.J., Mclaughin P.V., Sarmiento J.S., Youd, T.L. "Geotechnical Investigation of Liquefaction Sites, Imperial County, California.", United States department of the Interior Geological Survey, Open-File Report 84-252, Menlo Park: California, 1984.
14. Holzer T.L., Youd T.L., Bennet, M.J. "In situ Measurement of Pore Pressure Build-up During Liquefaction.", issued by NIST, Jan. 1989, Proceedings of the 20th Joint meeting of United States-Japan Panel on Wind and Seismic Effects, Gaithersburg, MD, 1988: 118–130.

15. Baziar M.H., Dobry R., Elgamal A.-W “Engineering evaluation of permanent ground deformations due to seismically-induced liquefaction.”, Tech. Rep. NCEER-92-0007, Nat. Ctr. For Earthquake Engrg. Res., SUNY-Buffalo, Buffalo, N.Y., 1992.
16. Cooke H.G., “GROUND improvement for liquefaction mitigation at existing highway bridges.”, Ph.D. dissertation, Virginia Polytechnic Institute and State University, Department of Civil Engineering, Blacksburg, VA, 2001.
17. Gu W.H., Morgenstern N.R., Robertson P.K. “Post earthquake deformation analysis of wildlife site.”, J. of Geotech. Engrg. 1994, 120(2), 274-289.
18. Itasca Consulting Group, Inc. “FLAC-Fast lagrangian analysis of continua.”, User’s Manuals for Version 4.0, Itasca Consulting Group, Inc., Minneapolis, MN, 2002.
19. Martin G. R., Finn W.D.L., Seed H. B., “Fundamentals of Liquefaction Under Cyclic Loading.” J. Geotech., Div. ASCE 1975, 101(GT5), 423-438.
20. Koohi S. “Modeling and numerical analysis of lateral spreading due to liquefaction.”, M. Sc. dissertation, Amirkabir university of Tehran, 2004.